Pediatric Radiology (2024) 54:1906–1918
https://doi.org/10.1007/s00247-024-06048-7

ORIGINAL ARTICLE

Biomarkers of mitochondrial stress and DNA damage during pediatric catheter-directed neuroangiography – a prospective single-center study

Kaley A. Hogarth[1,2] · Nicholas A. Shkumat[5,6] · Simal Goman[5] · Afsaneh Amirabadi[5] · Suzanne Bickford[5,7] · Prakash Muthusami[5,6,7] · Bairbre L. Connolly[5,6,8] · Jason T. Maynes[1,2,3,4]

Received: 2 May 2024 / Revised: 21 August 2024 / Accepted: 25 August 2024 / Published online: 17 September 2024

Abstract

Background Neuroangiography represents a critical diagnostic and therapeutic imaging modality whose associated radiation may be of concern in children. The availability of *in vivo* radiation damage markers would represent a key advancement for understanding radiation effects and aid in the development of radioprotective strategies.

Objective Determine if biomarkers of cellular damage can be detected in the peripheral blood mononuclear cells (PBMC) of children undergoing neuroangiography.

Materials and methods Prospective single-site study of 27 children. Blood collected pre and post neuroangiography, from which PBMC were isolated and assayed for biomarkers of mitochondrial stress (mitochondrial membrane potential (MMP), reactive oxygen species (ROS), and mitochondrial DNA (mtDNA)) and DNA damage (γH2AX). Dose response of biomarkers vs. radiation dose was analyzed using linear regressions. The cohort was divided into higher (HD) and lower dose (LD) groups and analyzed using linear mixed models and compared using Welch's *t*-tests.

Results No biomarker exhibited a dose-dependent response following radiation (γH2AX: $R^2 = 0.0012$, $P = 0.86$; MMP: $R^2 = 0.016$, $P = 0.53$; mtDNA: $R^2 = 0.10$, $P = 0.11$; ROS: $R^2 = 0.0023$, $P = 0.81$). Groupwise comparisons showed no significant differences in γH2AX or ROS after radiation (γH2AX: LD: 0.6 ± 6.0, $P = 0.92$; HD: -7.5 ± 6.3 AU, $P = 0.24$; ROS: LD: 1.3 ± 2.8, $P = 0.64$; HD: -3.6 ± 3.0 AU, $P = 0.24$). Significant changes were observed to mitochondrial markers MMP (-53.7 ± 14.7 AU, $P = 0.0014$) and mtDNA (-1.1 ± 0.4 AU, $P = 0.0092$) for HD, but not the LD group (MMP: 26.1 ± 14.7 AU, $P = 0.090$; mtDNA: 0.2 ± 0.4, $P = 0.65$).

Conclusions Biomarkers of mitochondrial stress in PBMC were identified during pediatric neuroangiography and warrant further investigation for radiation biodosimetry. However, isolating radiation-specific effects from those of procedural stress and general anesthesia requires further investigation.

Graphical Abstract

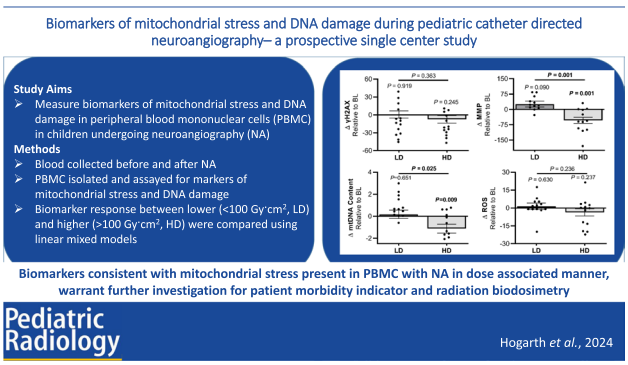

Extended author information available on the last page of the article

Keywords Mitochondria · Ionizing radiation · Interventional radiology · H2A histone family member X (H2AX) · Biomarkers

Introduction

Neuroangiography represents a critically important diagnostic and therapeutic imaging modality, enabling treatment of many complex neurovascular diseases. Despite many advantages (including minimal invasiveness, high spatial resolution, deep tissue access, avoidance of open surgery), these imaging procedures carry notable risks, as they typically employ ionizing radiation (hereafter referred to simply as radiation), which is epidemiologically linked to increased rate of both acute and chronic health problems [1–4]. Large-scale retrospective studies on radiation exposures have demonstrated increased incidence of cancer in children, who may be more sensitive than adults to the damaging effects of radiation due to a higher number of dividing cells and longer lifespans to express late effects [1, 5]. These findings prompted internationally endorsed programs (Image Gently, Step Lightly) promoting awareness for judicious use of radiation in pediatric imaging [6]. However, epidemiological studies have produced contradictory results, adding uncertainty to interpretation of radiation-associated risks [7]. While neuroangiography procedure volumes and their therapeutic potential increase, understanding the nature and cellular effects of radiation exposure has become paramount to mitigate potential lifelong consequences in children.

Although radiation's capacity to induce cellular damage has been frequently observed and described in human cells, both in vitro and ex vivo (see reviews [8–10]), uncertainty remains in modeling the relationship between exposure and detrimental biological consequences in vivo. Historically, physical measures of radiation dose (e.g., tube output, film) have been used to extrapolate risk of cellular damage and long-term health risks [11]. These models have inherent limitations, including assumptions based on a 70-kg "average" reference man [11]. To address these constraints, attention has turned to biodosimetry—methodologies which directly quantify biological effects of radiation at the cellular level *in vivo* and *ex vivo* to estimate dose [12]. Early biodosimetry techniques were manual, labor intensive, and error prone; newer automated techniques have made significant advancements, expanding their potential for prospective dose optimization [13].

Multiple candidate biodosimetry biomarkers have been proposed, targeting known cellular lesions of radiation exposure. Radiobiological dogma has predominantly stressed the nuclear genome as the primary site of radiation damage. Biomarkers measuring nuclear DNA damage have been investigated, given the correlation between radiation and cancers, and induction of genomic injuries observed *in vitro*. These markers include the phosphorylation of H2A histone family member X (H2AX) at serine 139 (γH2AX)—an essential step in the initiation of the DNA double-stranded break (DSB) repair processes in mammalian cells [14]. However, recent evidence suggesting that extra-nuclear sites may also bear a significant brunt of radiation's effects and thus contribute to the potential downstream consequences has generated additional biodosimetric candidates. One such site is the mitochondria, which have been shown to exhibit multiple lesions directly following radiation exposure including impaired oxidative phosphorylation, mitochondrial DNA (mtDNA) damage, excessive reactive oxygen species (ROS) generation, and altered mitochondrial membrane potential (MMP) [15–18]. Furthermore, radiation-induced injuries have also been proposed to mediate long-term cellular consequences, both directly (e.g., impaired energy production, excessive ROS production [17]) and indirectly (e.g., non-targeted/bystander effects [19–21]) making the mitochondria an attractive target as a biodosimetric marker for radiation injury.

Although biodosimetry holds tremendous clinical potential, ethical constraints necessitate that *in vitro* analyses contribute most to our current understanding of radiation response modeling, with many questions remaining regarding these responses *in vivo*. We sought to quantify the potential short-term cellular effects of radiation in peripheral blood mononuclear cells (PBMC) in children undergoing catheter-directed neuroangiography by measuring markers of DNA DSBs (γH2AX) and mitochondrial function (MMP, mtDNA, and ROS). Better understanding of cellular responses to radiation would represent an important step towards developing mitigation strategies and/or procedural guidelines for minimizing associated risks of neuroangiography procedures in the treatment of pediatric disease.

Materials and methods

Ethics approval and informed consent. Hospital Research Ethics Board approval was obtained and performed in accordance with the 1964 Declaration of Helsinki. The study was introduced to the patient/parents by the interventional radiologist. If interested, a clinical research associate not involved in the procedure explained the study and written informed consent was obtained.

Patient selection. This was a prospective study of 27 pediatric patients undergoing catheter-directed neuroangiography. These procedures were selected given the annual case volume, the broad range of potential exposures, requirement for magnification and high-resolution imaging, consistency of anatomic site and angles, and presence of an arterial sheath for sampling. Inclusion and exclusion criteria are outlined in Fig. 1. All procedures were performed in an interventional radiology suite (Artis Q, Siemens Healthineers, Erlangen, Germany) with real-time radiation dose index reporting and structured reports.

Study process. Blood samples (2 mL) were obtained once the arterial sheath was inserted (baseline) and immediately following the procedure (post-procedure). Samples were immediately time-stamped, placed on ice, and transported to the laboratory, where PBMC were isolated and assayed for markers of genomic and mitochondrial stress.

Biomarker selection and analysis. Analyzed biomarkers were chosen based both on their established use as markers of DNA damage and mitochondrial function and on their compatibility with rapid detection methods and cell type used in this study [22, 23]. PBMC were isolated using Ficoll-Paque™ Plus (GE Healthcare, Pittsburgh, PA, USA). MMP, ROS, and γH2AX in PBMC were measured with Muse MitoPotential, Oxidative Stress, and H2A.X Dual Activation kits respectively (Luminex, Austin, TX, USA). For mtDNA quantification, qPCR reactions were performed with SsoFast™ EvaGreen® Supermix in a Bio-Rad CFX96 Real-Time PCR Detection System (Hercules, CA, USA) using Geneaid Blood DNA Kit (New Taipei City, Taiwan) isolated genomic DNA and *nd1* and *gapdh* primers. See Supplemental File 1 for detailed methods.

Radiation dose. The air kerma-area product (P_{KA}) ($Gy{\cdot}cm^2$) was recorded from the angiographic control screen at the time of each sample collection. The elapsed time (minutes following baseline) and P_{KA} delivered at each sample collection were recorded. Radiation measurements were confirmed by correlation to finalized dosimetry measurements in the post-procedure radiation dose structured report. P_{KA} was used as the primary radiation quantity for analysis as it is a reproducible, measurable quantity independent of source-patient-detector geometry and incorporates field size (collimation), making it an appropriate surrogate measure for energy delivered to patients. Effective dose was not considered as it is, by definition, not a measurable quantity and is calculated for a reference person and should not be used for detailed specific retrospective investigations of individual exposure as stated by the International Commission on Radiological Protection [24].

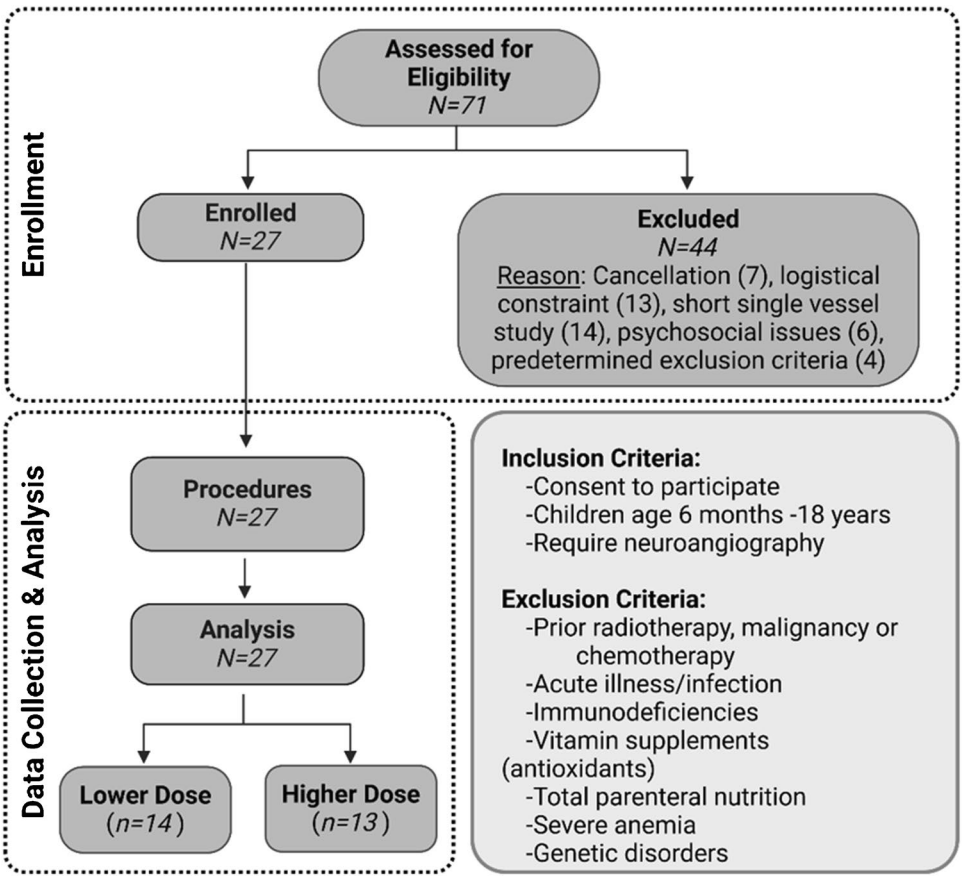

Fig. 1 Study enrollment flowchart and eligibility criteria. Created using biorender.com

Dose groups. For exploratory analysis of dose-association, patients were also divided into two groups defined by their cumulative P_{KA}. A threshold value of 100 Gy·cm^2 was applied to delineate lower dose (LD, $P_{KA} < 100$ Gy·cm^2) from higher dose (HD, $P_{KA} > 100$ Gy·cm^2) exposure groups. The cut-off value of 100 Gy·cm^2 was chosen as this represents a commonly referenced clinical threshold prior to triggering additional dose management actions [25].

Statistical analysis. Statistical analysis was performed using GraphPad (Boston, MA, USA) Prism 9.0 and R Statistical Software version 4.1.1. Results are shown as mean ± standard deviation (SD). All statistical tests applied significance level of $\alpha = 0.05$ and a P-value significance threshold of < 0.05. Normality of distributions was tested with the D'Agostino and Pearson test. Baseline relationships between patient demographic features and biomarkers were assessed with simple linear regressions (for continuous variables) and unpaired t-test with Welch's correction (for categorical variables). To evaluate the dose-dependent/linear association between radiation dose and biomarker response, we performed simple linear regression analysis. Differences between exposure group characteristics at baseline were tested using unpaired t-test with Welch's correction (for normally distributed means), Mann–Whitney (non-normal distributed means), and Fisher's exact test (for ratios). To analyze the dose association of the biomarker response, we performed mixed-effects linear analysis between the dose groups using the lmer R function (lme4 package) in R [26, 27]. Mixed-models were used to account for random effects of multiple sampling experimental structure, as well as baseline differences in age and weight between groups. Models were fit with restricted maximum likelihood and evaluated by examining residual plots for homoscedasticity and normality. Each model included exposure group and collection point as explanatory variables. The models adjusted for patient age and weight as fixed effects, and patient number as random effect. Group means and post-hoc comparisons via two-sided Welch's t-tests were estimated with emmeans R function (emmeans package) [28]. Unless otherwise stated, data were presented as means ± standard deviation (SD) or medians with interquartile range (IQR).

Figure production. Figures were created using GraphPad Prism 9.0 and biorender.com.

Results

Participant characteristics. A total of 27 patients were enrolled (12 male, 15 female), with a mean age of 12.1 ± 4.4 years and weight of 49.0 ± 21.2 kg. Participant enrollment process and demographic features are summarized in Fig. 1 and Table 1, respectively, with individual participant features available in Supplemental File 2. We observed no acute adverse effects in the cohort over the study period.

Baseline biomarker characteristics. Biomarkers of mitochondrial function (MMP, ROS, mtDNA) and DNA DSB repair (γH2AX) had detectable and normally distributed signals at baseline. We observed no statistically significant predictive relationships between γH2AX, MMP, ROS, or mtDNA content and patient demographic features (age, weight, sex) (Fig. 2). Linear regression models and statistic summary available in Supplemental File 2.

Radiation dose response. We observed no statistically significant linear relationships between radiation dose and any of the measured biomarkers of DSB ($R^2 = 0.0012$, $P = 0.86$) or mitochondrial function (MMP: $R^2 = 0.016$, $P = 0.53$; mtDNA: $R^2 = 0.10$, $P = 0.11$; ROS: $R^2 = 0.0023$, $P = 0.81$) (Fig. 3). Linear regression models are available in Supplemental File 2.

Exposure group creation and characteristics. Applying a 100 Gy·cm^2 cut-off created two roughly equal-sized groups (LD: $N = 14$, HD: $N = 13$), which significantly differed in their P_{KA} post-procedure (LD: 64.20 (35.30)

Table 1 Demographic characteristics and procedure parameters of study population

	N	Range	Mean ± SD	Median + IQR
Age (years)	-	2.0–18.0	12.1 ± 4.4	-
Weight				
kg	-	14.0–99.0	49.0 ± 21.2	-
pc	-	0.7–98.7	61.1 ± 32.0	-
Sex				
Male	12	-	-	-
Female	15	-	-	-
Total procedure time (min)	-	18.0–273.0	108.8 ± 81.3	-
Total procedure P_{KA} (Gy·cm^2)	-	35.0–477.0	-	92.0 + 135.0

Mean values (± SD) presented for normally distributed data, median (± IQR) for non-normal according to D'Agostino and Pearson test. *SD*, standard deviation; P_{KA}, air kerma-area product; *IQR*, interquartile range; *pc*, percentile

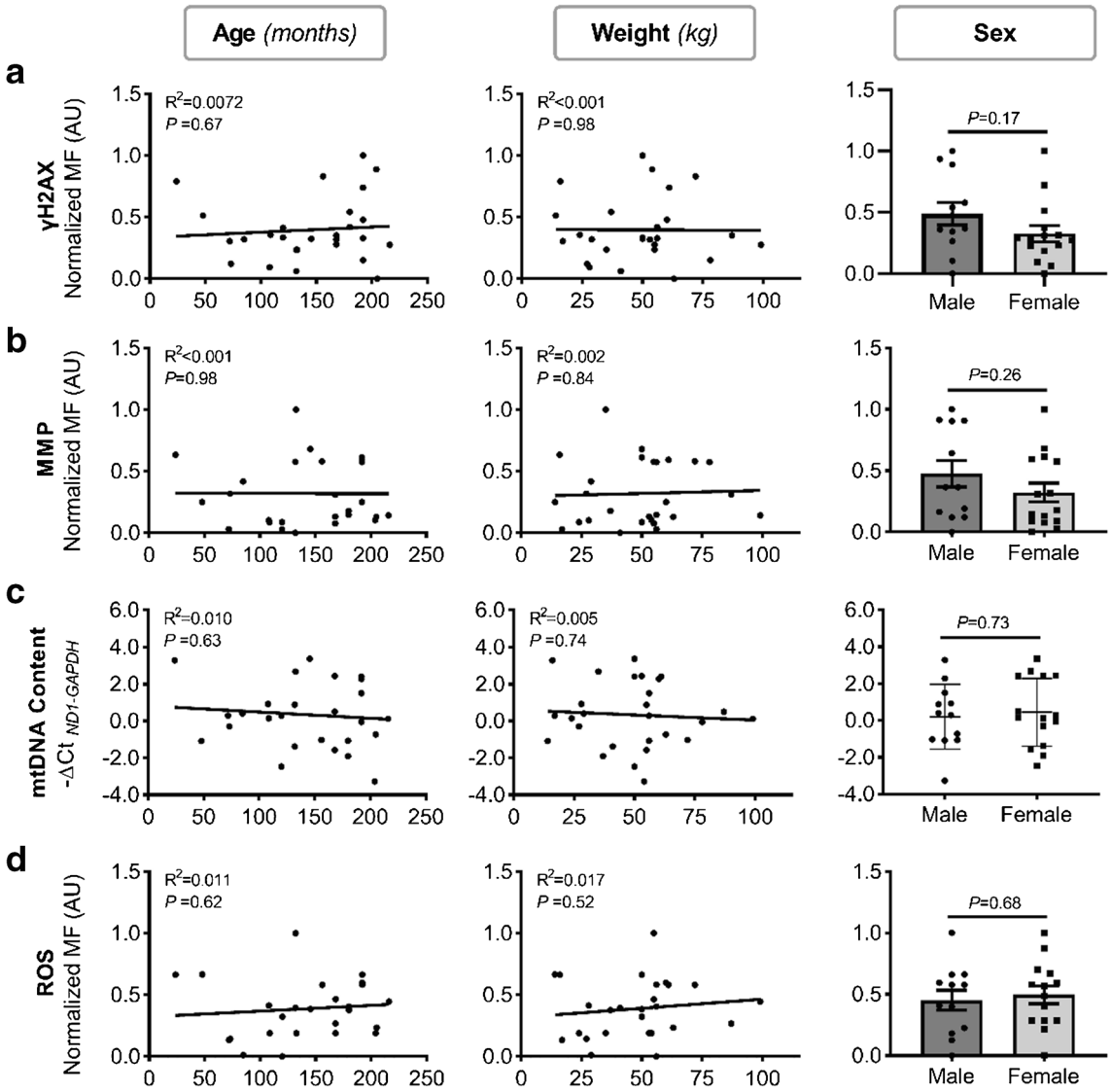

Fig. 2 Baseline patient demographics and biomarker relationships. No significant predictive relationships between patient demographic features and tested biomarkers (**a**) γH2AX, **b** MMP, **c** mtDNA, and (**d**) ROS were observed at baseline in patient peripheral blood mononuclear cells. Individual samples appear as *single dots*, with *bars* representing means and *error bars* standard deviation. *Solid lines* indicate simple linear regressions. Mean fluorescence (MF), arbitrary units (AU), serine 139 H2A histone family member X (γH2AX), mitochondrial membrane potential (MMP), reactive oxygen species (ROS), and mitochondrial DNA (mtDNA)

Gy·cm^2, HD: 198.20 (128.90) Gy·cm^2, $P < 0.001$), but not in elapsed time (LD: 88.64 ± 71.69 min, HD: 130.50 ± 89.19 min, $P = 0.19$) (Fig. 4). The groups significantly varied in age (LD: 10.03 ± 4.79 years, HD: 14.24 ± 2.38 years, $P = 0.009$) and weight (LD: 38.00 ± 17.69 kg, HD: 60.85 ± 18.59 kg, $P = 0.003$), but not in male–female ratio (LD: 1.33, HD: 0.44, $P = 0.25$) (Fig. 4). No differences between groups were observed at baseline for γH2AX (LD: 138.2 ± 15.43 AU, HD: 143.30 ± 15.66 AU, $P = 0.52$), ROS (LD: 105.60 ± 8.38 AU, HD: 112.40 ± 7.77 AU, $P = 0.074$), MMP (LD: 475.00 ± 43.20 AU, HD: 513.3 ± 56.02 AU, $P = 0.085$) signal, or mtDNA (LD: 0.47 ± 1.87, HD: 0.18 ± 1.73, $P = 0.64$) (Fig. 5).

Exposure group DSB biomarker following radiation. We observed no significant changes in γH2AX levels relative to baseline in either exposure group (LD: 0.6 ± 6.0 AU, $P = 0.92$; HD: -7.5 ± 6.3 AU, $P = 0.24$), or difference between the groups (8.1 ± 8.7 AU, $P = 0.36$) (Fig. 6a).

Exposure group mitochondrial biomarkers following radiation. Following radiation, the HD group demonstrated a concurrent decrease in MMP (-53.7 ± 14.7 AU,

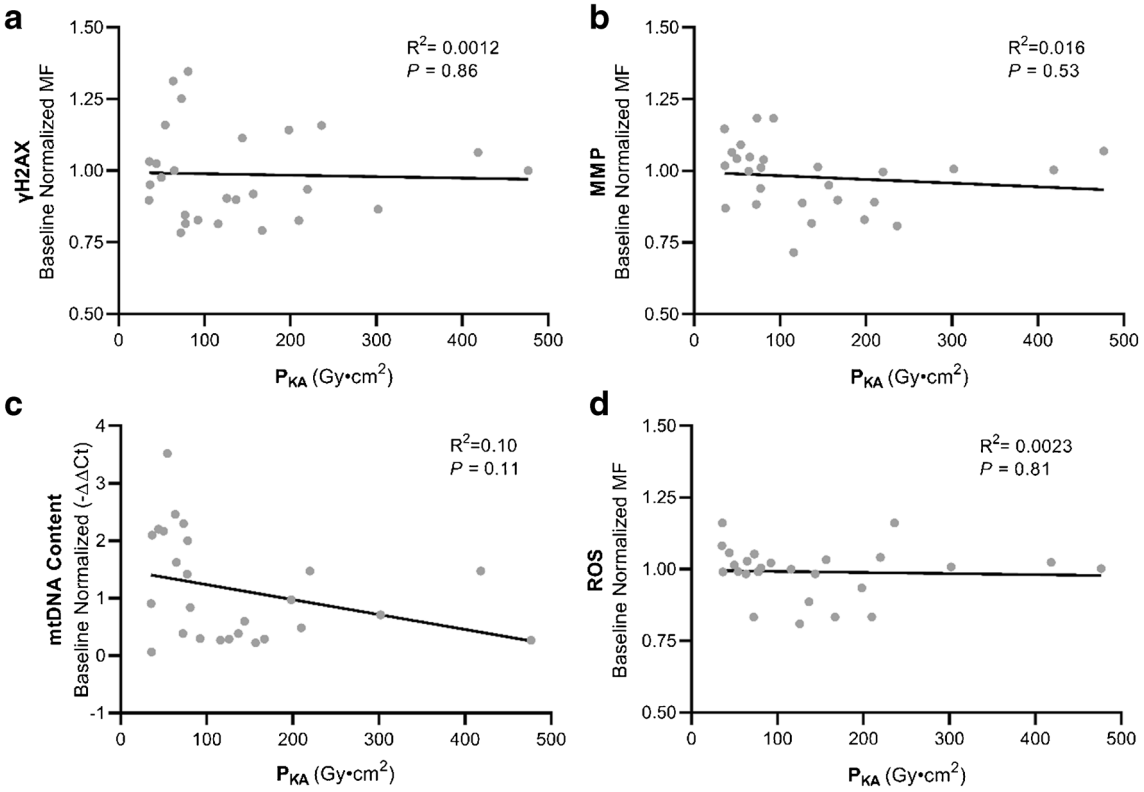

Fig. 3 Biomarker response following radiation exposure. No significant dose-dependent relationships between radiation dose and tested biomarkers (**a**) γH2AX, **b** MMP, **c** mtDNA, and (**d**) ROS were observed in patient peripheral blood mononuclear cells following neuroangiography procedures. *Solid lines* indicate simple linear regressions, with individual samples appearing as *single dots*. Mean fluorescence (MF), serine 139 H2A histone family member X (γH2AX), mitochondrial membrane potential (MMP), reactive oxygen species (ROS), and mitochondrial DNA (mtDNA)

$P=0.0014$) and mtDNA content (-1.1 ± 0.4 AU, $P=0.0092$) from baseline levels, which significantly differed from the LD group (MMP: 79.8 ± 20.8 AU, $P=0.001$; mtDNA: -1.3 ± 0.5, $P=0.025$). While the LD group exhibited modest increases in both MMP (26.1 ± 14.7 AU, $P=0.090$) and mtDNA (0.17 ± 0.38, $P=0.65$), neither of these changes was statistically significant from baseline levels. We observed no statistically significant changes in ROS levels for either the LD (1.3 ± 2.8 AU, $P=0.64$) or HD groups (-3.6 ± 3.0 AU, $P=0.24$), or differences between groups (5.0 ± 4.1 AU, $P=0.24$) (Fig. 6d).

Discussion

With the tremendous therapeutic benefit that neuroangiography and neurointervention provide, understanding the impact of clinically relevant radiation exposure is vital when developing usage guidelines and standard practices to best weigh the benefits and potential consequences. This balance is especially critical in children given their combination of enhanced radiosensitivity and remaining life span to express radiation-induced damage. Traditional markers of radiation damage have typically required technically challenging and time-intensive methods, limiting their applicability. This study investigated biomarkers of mitochondrial function and DNA DSB repair following neuroangiography radiation exposure in pediatric patients, using rapid semi-automated detection methods.

Substantial evidence in both *in vitro* and *in vivo* models has demonstrated the capacity for radiation to inflict damage to the nuclear genome, including DSBs. With such deleterious potential, DSBs were historically considered among the most destructive effects of radiation, resulting in research focused on biomarkers that reflect these lesions, such as γH2AX. Consistent with previous works, we observed detectible, normally distributed levels of γH2AX signal at baseline, reflective of its ongoing role in the initiation of DSB repair pathway from all sources of DNA damage under normal physiological conditions, not just radiation induced [13, 29, 30]. In contrast to adult studies reporting age-dependent increases in γH2AX, we did not observe any age dependency in γH2AX levels [13]. This observation may be due to the narrow pediatric age range; however, Belmans

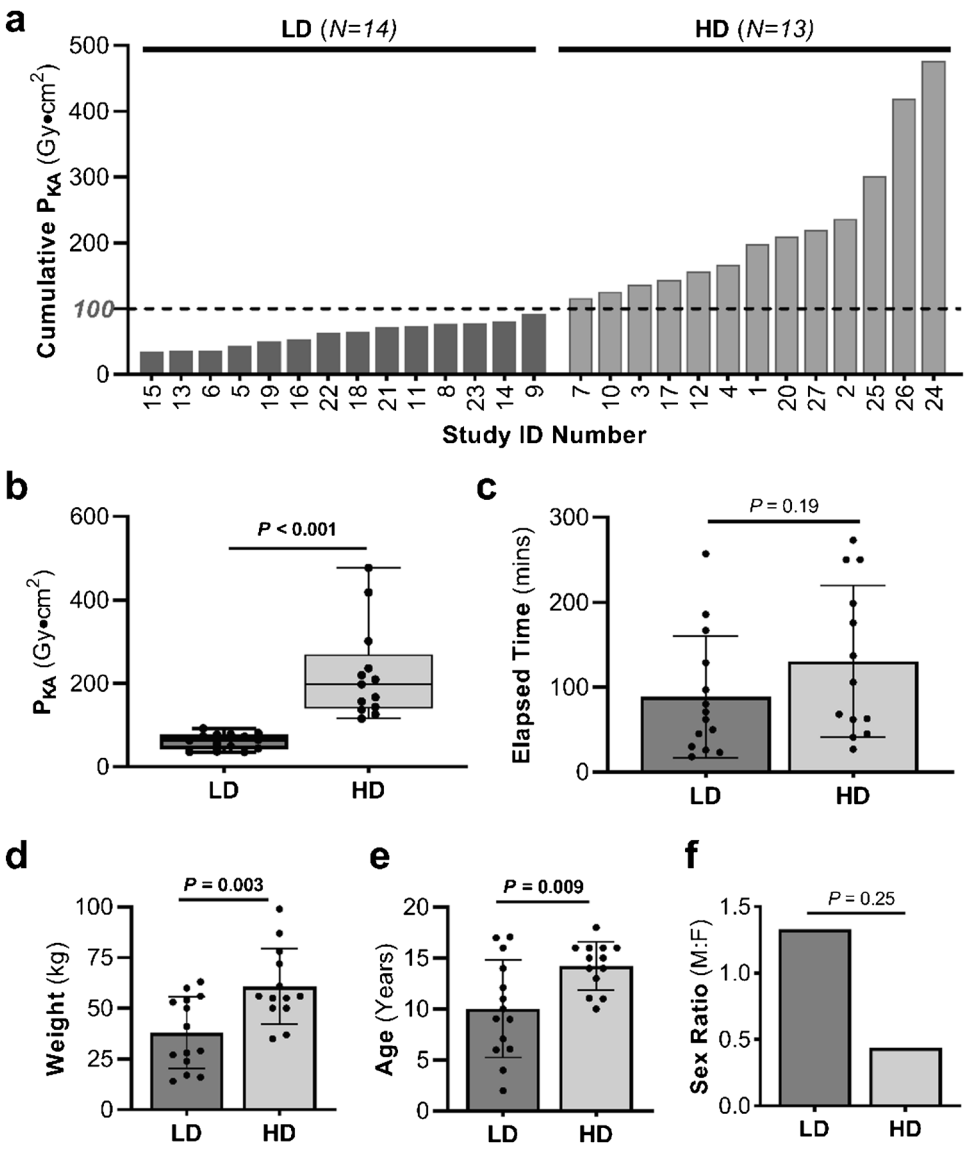

Fig. 4 Exposure group participant and procedural features. Cumulative P_{KA} for each patient arranged in ascending order to demonstrate group compositions, with cut-off value demarcating the HD and LD groups represented with *dotted line* (**a**). HD and LD groups did not differ significantly in elapsed time (**c**) but did vary in cumulative P_{KA} (**b**). Weight (**d**) and age (**e**) significantly differed between the LD and HD groups, while the male–female ratio did not (**f**). Individual samples appear as *single dots*, with *bars* representing means and with *error bars* standard deviation. *Box-and-whisker plots* show upper quartile (*top line*), median (*middle line*), and lower quartile (*bottom line*) with upper and lower extreme whiskers. Lower dose (LD), higher dose (HD), air kerma-area product (P_{KA}), male (M), and female (F)

et al. [31] observed that children had statistically higher levels of DSBs than adults at baseline in buccal mucosal samples. This highlights potential differences between adults and children in baseline DNA damage repair and susceptibility to radiation.

We observed no significant changes to γH2AX following radiation in either dose group. Although the range of radiation used here has been shown in various cell types (including PBMC) to induce DSBs *in vitro*, results *in vivo* have been mixed, some observing significant increases in γH2AX [32, 33], others observing no changes following radiology procedures, including neuroangiography [31, 34–36]. Differences in observations have been attributed to a few sources. Optimistically, our results may demonstrate that there are no statistical increases in DNA DSBs in PMBC at the studied dose range. However, despite observing no changes to γH2AX, Basheerudeen *et al.* [35] observed statistical increases in chromosomal abnormalities and micronuclei, cautioning isolated interpretation of γH2AX levels. γH2AX signal is contingent on two overlapping processes, formation and removal, leaving the assay vulnerable to temporal dynamics of biphasic DNA repair. γH2AX levels are significantly modified by the radiation exposure (dose timing, location, rate, etc.) as well as individual factors (age, race, environmental exposures, etc.) which are partially accounted for in our procedural (length, exposure location, etc.) and patient inclusion criteria (age, comorbidities, etc.) [13, 37, 38]. While our experimental design precludes us determining if our observations are due to lack of any increase in γH2AX, or missing its increase window, it is notable that γH2AX signal in PBMC remains stable up to 5 hrs when stored on ice (as in our protocol) and other reports have observed DNA breaks at doses at or below those used here [31, 33, 36, 39–41].

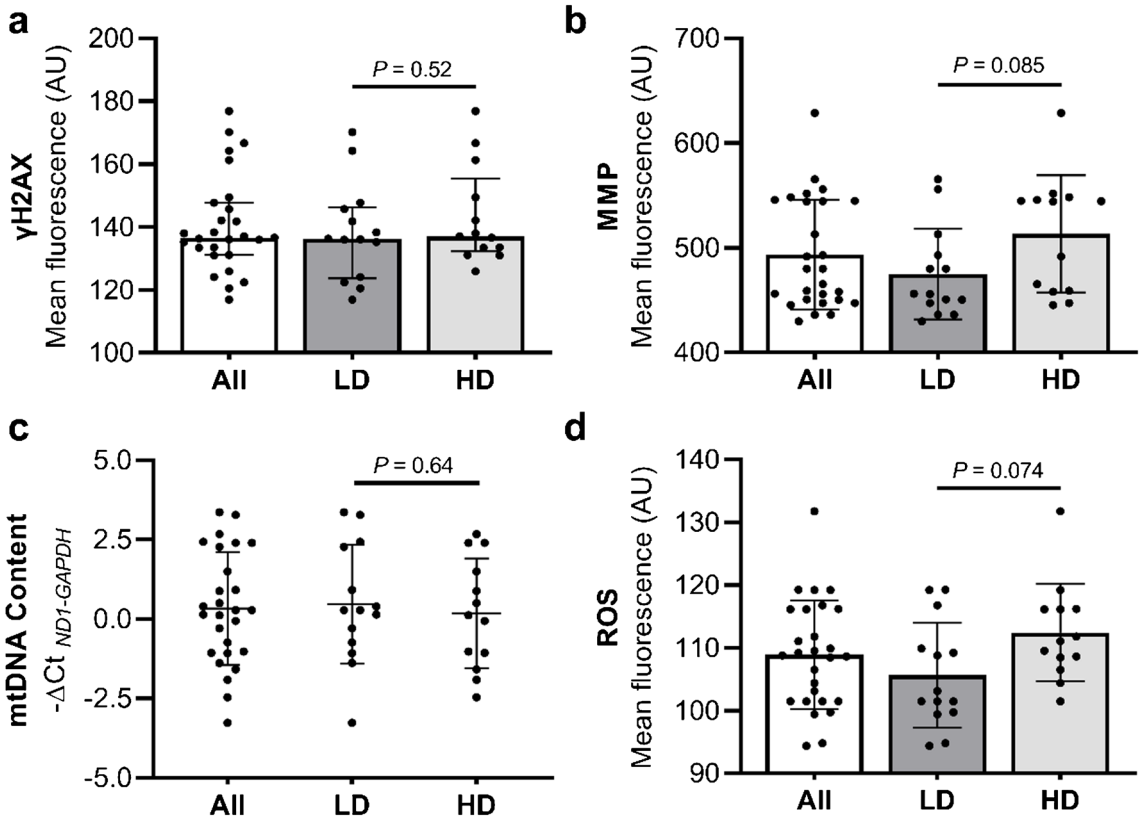

Fig. 5 Peripheral blood mononuclear cell biomarker levels at baseline. No differences between the HD and LD groups were observed in (**a**) γH2AX, **b** MMP, **c** mtDNA, or (**d**) ROS. Individual samples appear as *single dots*, with *bars* representing means and with *error bars* SD. Lower dose (LD), higher dose (HD), arbitrary units (AU), serine 139 H2A histone family member X (γH2AX), mitochondrial membrane potential (MMP), reactive oxygen species (ROS), and mitochondrial DNA (mtDNA)

While DNA DSBs are among the most mutagenic and severe radiation-induced lesions, accumulating evidence suggests that extra-nuclear targets (e.g., mitochondria) contribute to the damaging downstream effects of radiation exposure [15–17, 42]. Mitochondria participate in many cellular functions, including mediating and energetically fueling responses to radiation damage, making impairments to their functional capacity devastating for the cell. Mitochondria, occupying approximately 25–30% of cytoplasmic volume, may be exposed to more ionization events for a given radiation dose than the nuclear compartment [15, 43]. Our HD group exhibited loss of MMP following radiation which has also been observed in human U987 [44], dermal fibroblasts [45], MCF-7 [18], and HEK [46] cells following *in vitro* radiation exposure, and *in vivo* mouse PBMC [47]. Depolarization is considered an indication of dysfunction as mitochondria require a highly charged membrane potential for full functionality. A loss of this polarization state can be accompanied with functional consequences (e.g., reduced energy production and increased ROS generation) and the initiation of processes like mitophagy and apoptotic cell death [15, 16, 42].

In addition to changes in MMP, the HD group also exhibited a decrease in mtDNA, indicating damage from loss of mitochondrial mass through mitophagy. Without the protection and repair systems afforded to the nuclear genome, mtDNA has demonstrated enhanced sensitivity to radiation compared to its nuclear counterpart, making this reduction in the HD group logically consistent [15–17, 42, 45]. The LD group exhibited a slight trend towards increased mtDNA which was statistically higher than the HD group, similar to results *in vitro* radiation exposures in human fibroblasts [45], HTC116 [48], and *in vivo* with *Caenorhabditis elegans* [49] and mice [50], though the causes for this increase remain unknown. It has been proposed that this elevation represents a compensatory response to maintain mitochondrial function following radiation-induced damage [51] and that an increase in DNA–protein complexes may physically shield/protect intact mtDNA from direct ROS contact [50]. If indeed increased mtDNA is adaptive, the divergent response between HD and LD groups suggests a fundamental difference in cellular response mechanism induced by differing levels of radiation.

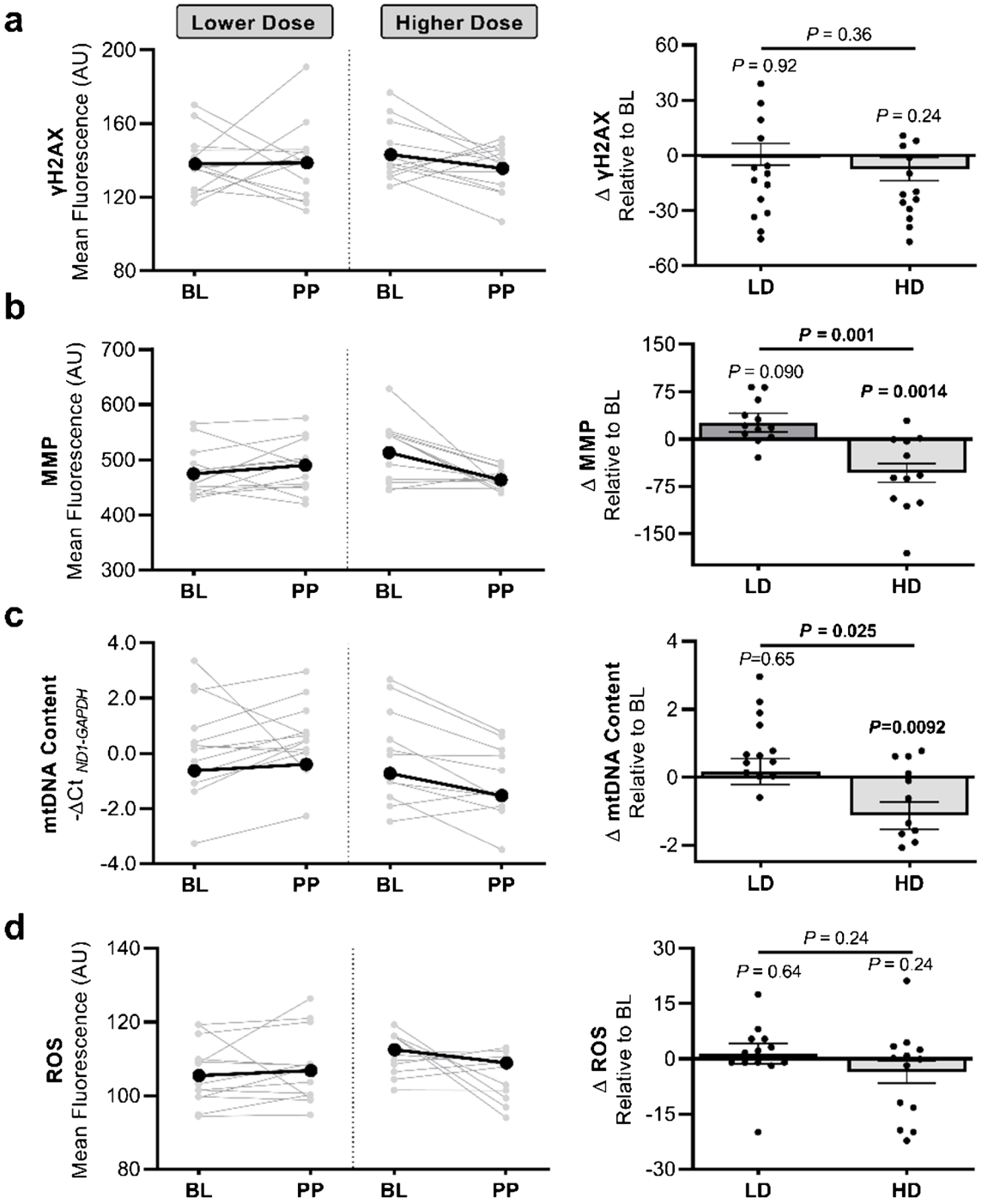

Fig. 6 Peripheral blood mononuclear cell response to radiation exposure. The HD group showed significant reductions in (**b**) MMP, coupled with (**c**) decreased mtDNA content compared to baseline (BL) values, and relative to the LD group post-procedural (PP). Neither group exhibited changes in (**d**) ROS or (**a**) γH2AX levels from baseline or between the groups. *Black solid lines* represent group means, and *gray* indicate individual signals (*left*). *Bars* represent mixed-effects model estimates, with standard error of the mean in *error bars* (*right*). *P*-values above *black line* denote comparisons made between groups, while the *P*-values above each *bar* indicate the comparison to baseline values. Lower dose (LD), higher dose (HD), arbitrary units (AU), serine 139 H2A histone family member X (γH2AX), mitochondrial membrane potential (MMP), reactive oxygen species (ROS), and mitochondrial DNA (mtDNA)

We observed no changes in ROS levels following radiation exposure. Although functionally essential, excessive ROS can induce cellular lesions, making ROS regulation a critical homeostatic process, balancing its physiological role and pathophysiological potential. Due to their extreme reactivity and rapid neutralization mechanisms, cellular ROS levels are difficult to directly measure in biological samples, making detection of ROS damage or antioxidant response more commonly used as surrogate ROS markers [52]. Such markers have been commonly used to demonstrate increases in oxidative damage in both in vitro and in vivo reports [19, 52, 53]. While radiation can produce ROS directly via hydrolysis, these radicals are typically short lived and represent the minority of total ROS following radiation [15, 54]. Most radiation-induced ROS, produced by damaged mitochondria, take hours-days to produce detectable changes [19, 42, 44]. Taken together, while it is possible that our results indicate no IR induced ROS increases, it is also conceivable that the sampling points used were unable to capture either the short-lived radiation-induced or mitochondrial-derived ROS, which take longer to appear.

While central radiobiological dogma suggests that radiation's primary target is nuclear DNA, there is mounting evidence that suggests that nuclear damage is secondary to mitochondrial injury [15–17]. Our results may support the theory that mitochondria are both the target and key regulators in mediating radiation-associated damage, including DNA DSB [15–17]. It is hypothesized that radiation causes physical damage to mitochondria and mtDNA, resulting in MMP loss and increased mtDNA damage, as observed in the HD group. While performing oxidative phosphorylation to meet the energetic demand to fuel necessary repair processes (including DSB repair), damaged mitochondria produce excessive oxygen radicals, further increasing total cellular ROS. This feedback loop promotes a cycle of ROS production and ROS mediated cellular damage, causing further cellular lesions including DSBs. This hypothesis could explain the lack of ROS or γH2AX elevation in either exposure group, as ROS accumulation from dysfunctional mitochondria requires time beyond our sampling to elevate and inflict DNA damage. Results in the HD group possibly support this hypothesis, which showed evidence of radiation inducing a mitochondrial response, but no ROS or γH2AX elevation. While preliminary, our results may support the use of mitochondrial radioprotectants for pediatric patients undergoing radiation-based treatments. Investigations into agents targeting mitochondrial protection, including epicatechin and epigallocatechin-3-gallate, have been shown to prevent radiation-induced cellular lesions including reduced cellular ROS level, apoptosis, and γH2AX foci development, as well as increased mitochondrial integrity and mitochondrial antioxidant expression [55, 56].

The LD exposure group showed no significant response to radiation from baseline. Whether this reflects a lack of cellular damage in these dose conditions, or limits of the assay sensitivity to detect changes at these doses, requires further validation. The linear non-threshold model implies no minimum dose where a linear dose-biological effect of radiation does not exist [57]. This model is challenged, especially at lower ranges of the radiation spectrum, because of lack of consideration of biological protective mechanisms, e.g., DNA repair [57, 58]. Furthermore, studies have shown biologically distinct responses between high- and low-dose exposures, such as divergent shifts in mitochondrial morphology, apoptosis initiation, and γH2AX foci formation [47, 59]. This highlights the complexities of radiation exposure effects on humans, supporting further investigation.

As is true for all applications of ionizing radiation in medicine, the dose should be limited to only what is appropriate to achieve the clinical task. In interventional neuroangiography, patient dose optimization requires a multifaceted combination of operator, equipment, and technological considerations. These include but are not limited to the customization of technical protocols for pediatric use, application of advanced digital image processing, reduced use of high dose-rate and high-level techniques, appropriate collimation, limited (targeted) use of cone-beam CT, thorough equipment commissioning, routine quality evaluations, and extensive training/certification of interventional radiologists [6, 60–62]. Continuous radiation dose index monitoring and the development and implementation of a patient follow-up and consultation mechanism are also essential for complex interventions [6, 60–62].

The quantity of radiation applied in neuroangiography is dependent primarily on procedure complexity and vascular anatomy, unlike in chest or abdominal angiography where patient habitus and its variability are also significant contributors. Radiation risk is dependent on numerous elements including the radiation dose and dose rate, organs receiving radiation, patient age, and individual factors pertaining to each patient [63]. Further, assessing risk is complex, notably in children due to variability in size of the patient and individual organs, growth patterns, and differences in hormonal and endocrine activity, among other factors [63]. This work sought to understand the feasibility of assessing if peripheral blood mononuclear cells could represent a potential dosimetric tool for monitoring the effects of ionizing radiation to better understand these behaviors.

There are multiple limitations to this preliminary study which should be acknowledged for appropriate interpretation of our results. Our sample size was limited (although significant for pediatric studies), requiring larger scale studies for validation. Timing of sample collection, which was chosen to minimize procedural interference and maximize patient safety, impacted the ability to capture the complexities of

temporally sensitive events and should be expanded in future research to include multiple sampling points to better inform the evolution of radiation response and optimal response timepoint. The inclusion criteria, allowing a wide range in patient age (2–18), combined with small numbers, and by chance a larger proportion of older children, precluded identifying potential unique susceptibilities and responses to radiation exposure within different age groups. We assessed biomarkers in PBMC using established protocols and minimal patient invasiveness; however, the translation of local damage to systemic/circulatory stress is not fully understood. Additionally, the use of circulating PMBC resulted in only a fraction of the total cell population being exposed to the radiation field at any one time. Lastly, the non-standardized anesthetic regimens may represent a source of inter-individual variability in cellular stress, as general anesthetics can induce multiple cellular lesions including mitochondrial [64] and endoplasmic reticulum [65] dysfunction. Although not entirely standardized, all patients received a sevoflurane and narcotic-based anesthetic, substantially reducing the potential of the anesthetic in effecting our results.

Future investigations would benefit from including additional post-procedural collection points (e.g., 12/24/48 h or days/weeks post-radiation) to better understand the temporal evolution of the radiation response at both acute and chronic phases. While there were no observable short-term adverse effects identified in this cohort, expanding monitoring/collection point sampling may allow correlation between biomarkers and post-procedural outcomes, including assessment of long-term risk. Inclusion of other sample types in our analysis (e.g., buccal mucosal cells) would be informative to understand local vs. general effects of radiation exposure. Additionally, our results suggest that the use of protective agents may be appropriate to mitigate radiations effects, which warrant future investigation.

This work described the radiation response in a sample of pediatric patients undergoing neuroangiography using multiple biomarkers in PBMC. Dose assessment strategies are critical for monitoring cellular response to radiation exposure, and evaluating the effectiveness of protective strategies, which optimally balance sufficient dose and acceptable toxic health effects. To this end, our results add another aspect in our understanding and ability to monitor cellular responses to radiation exposure, as well as support the potential use of mitochondrial-targeted radioprotectants.

Conclusion

This study provides preliminary evidence that biomarkers of mitochondrial stress in peripheral blood mononuclear cells are detected at radiation exposure levels encountered during clinical pediatric neuroangiography. However, isolating radiation-specific effects from those of procedural stress and general anesthesia requires further investigation.

Supplementary Information The online version contains supplementary material available at https://doi.org/10.1007/s00247-024-06048-7.

Acknowledgements JTM would like to thank the members of the Department of Anesthesia and Pain Medicine at the Hospital for Sick Children (Toronto, ON, Canada) for the protection of research time and the Joseph and Groves Families and SickKids Foundation as the holder of the Curtis Joseph and Harold Groves Chair in Anesthesia and Pain Medicine. This work was made possible with funding from the Society for Pediatric Radiology Foundation and their support was greatly appreciated. We would like to thank members of the interventional team who assisted with blood sampling during neuroangiography.

Author contribution Conceptualization: J.M., B.C. Supervision: J.M., B.C. Procedures performed: P.M. Data collection: K.H., N.S., S.G., S.B., A.A. Data analysis: K.H., J.M., N.S. Original draft: K.H., J.M. Review and editing: J.M., B.C., N.S., P.M., S.G., S.B., A.A. Funding acquisition: J.M., B.C. All authors reviewed and approved the final version of the manuscript.

Funding Funding for this research was provided by SickKids Foundation and the Society for Pediatric Radiology.

Data availability Data from this study are not openly available due to reasons of sensitivity and are available from the corresponding author upon reasonable request. Data are located in controlled access data storage at SickKids Research Institute.

Declarations

Ethics approval The study received approval from the Research Ethics Board of the Hospital for Sick Children. All procedures were performed in accordance with the ethical standards of the Declaration of Helsinki.

Consent Written informed consent was obtained from all individual participants included in this study, or their parents/legal guardians.

Conflicts of interest None

References

1. Abalo KD, Rage E, Leuraud K et al (2021) Early life ionizing radiation exposure and cancer risks: systematic review and meta-analysis. Pediatr Radiol 51:45–56
2. Raelson CA, Kanal KM, Vavilala MS et al (2009) Radiation dose and excess risk of cancer in children undergoing neuroangiography. Am J Roentgenol 193:1621–1628
3. Chaparian A, Zarchi HK (2018) Assessment of radiation-induced cancer risk to patients undergoing computed tomography angiography scans. Int J Radiat Res 16:107–115
4. Shen J, Karki M, Jiang T, Zhao B (2018) Complications associated with diagnostic cerebral angiography: a retrospective analysis of 644 consecutive cerebral angiographic cases. Neurol India 66:1154–1158
5. Huang WY, Muo CH, Lin CY et al (2014) Paediatric head CT scan and subsequent risk of malignancy and benign brain tumour: a nation-wide population-based cohort study. Br J Cancer 110:2354–2360
6. Sidhu M, Coley BD, Goske MJ et al (2009) Image Gently, Step Lightly: increasing radiation dose awareness in pediatric interventional radiology. Pediatr Radiol 39:1135–1138

7. Jánošíková L, Juričeková M, Horváthová M et al (2019) Risk evaluation in the low-dose range CT for radiation-exposed children based on DNA damage. Radiat Prot Dosim 186:163–167
8. Reisz JA, Bansal N, Qian J et al (2014) Effects of ionizing radiation on biological molecules - mechanisms of damage and emerging methods of detection. Antioxid Redox Signal 21:260–292
9. Maier P, Hartmann L, Wenz F, Herskind C (2016) Cellular pathways in response to ionizing radiation and their targetability for tumor radiosensitization. Int J Mol Sci 17:102
10. Jiao Y, Cao F, Liu H (2022) Radiation-induced cell death and its mechanisms. Health Phys 123:376–386
11. Miller DL, Kwon D, Bonavia GH (2009) Reference levels for patient radiation doses in interventional radiology: proposed initial values for U.S. practice. Radiology 253:753–764
12. Swartz HM, Williams BB, Flood AB (2014) Overview of the principles and practice of biodosimetry. Radiat Environ Biophys 53:221–232
13. Raavi V, Basheerudeen SAS, Jagannathan V et al (2016) Frequency of gamma H2AX foci in healthy volunteers and health workers occupationally exposed to X-irradiation and its relevance in biological dosimetry. Radiat Environ Biophys 55:339–347
14. Paull TT, Rogakou EP, Yamazaki V et al (2000) A critical role for histone H2AX in recruitment of repair factors to nuclear foci after DNA damage. Curr Biol 10(15):886–895
15. Kam WWY, Banati RB (2013) Effects of ionizing radiation on mitochondria. Free Radic Biol Med 65:607–619
16. Szumiel I (2015) Ionizing radiation-induced oxidative stress, epigenetic changes and genomic instability: the pivotal role of mitochondria. Int J Radiat Biol 91:1–12
17. Averbeck D, Rodriguez-Lafrasse C (2021) Role of mitochondria in IR responses: epigenetic, metabolic, and signaling impacts. Int J Mol Sci 22:11047
18. Walsh DWM, Siebenwirth C, Greubel C et al (2017) Live cell imaging of mitochondria following targeted irradiation in situ reveals rapid and highly localized loss of membrane potential. Sci Rep 7:1–11
19. Azzam EI, Jay-Gerin JP, Pain D (2012) Ionizing radiation-induced metabolic oxidative stress and prolonged cell injury. Cancer Lett 327:48–60
20. Buonanno M, De Toledo SM, Pain D, Azzam EI (2011) Long-term consequences of radiation-induced bystander effects depend on radiation quality and dose and correlate with oxidative stress. Radiat Res 175:405–415
21. Miranda S, Correia M, Dias AG et al (2020) Evaluation of the role of mitochondria in the non-targeted effects of ionizing radiation using cybrid cellular models. Sci Rep 10:6131. https://doi.org/10.1038/s41598-020-63011-w
22. Kopp B, Khoury L, Audebert M (2019) Validation of the γH2AX biomarker for genotoxicity assessment: a review. Arch Toxicol 93:2103–2114
23. Hubens WHG, Vallbona-Garcia A, de Coo IFM et al (2022) Blood biomarkers for assessment of mitochondrial dysfunction: an expert review. Mitochondrion 62:187–204
24. The 2007 Recommendations of the International Commission on Radiological Protection. ICRP publication 103. Ann ICRP 37:1–332
25. Hirshfeld JW, Balter S, Brinker JA et al (2004) ACCF/AHA/HRS/SCAI clinical competence statement on physician knowledge to optimize patient safety and image quality in fluoroscopically guided invasive cardiovascular procedures: a report of the American College of Cardiology Foundation/American Heart Ass. J Am Coll Cardiol 44:2259–2282
26. RStudio Team (2020) RStudio: Integrated Development for R. In: RStudio. http://www.rstudio.com/. Accessed 22 June 2020
27. Bates D, Mächler M, Bolker B, Walker S (2015) Fitting linear mixed-effects models using lme4. J Stat Softw 67(1):1–48
28. Lenth R, Bolker B, Buerkner P, et al (2023) emmeans: estimated marginal means, aka least-squares means. https://cran.r-project.org/web/packages/emmeans/index.html. Accessed 22 June 2020
29. Roch-Lefèvre S, Mandina T, Voisin P et al (2010) Quantification of γ-H2AX foci in human lymphocytes: a method for biological dosimetry after ionizing radiation exposure. Radiat Res 174:185–194
30. Ismail IH, Wadhra TI, Hammarsten O (2007) An optimized method for detecting gamma-H2AX in blood cells reveals a significant interindividual variation in the gamma-H2AX response among humans. Nucleic Acids Res 35:e36. https://doi.org/10.1093/nar/gkl1169
31. Belmans N, Gilles L, Vermeesen R et al (2020) Quantification of DNA double strand breaks and oxidation response in children and adults undergoing dental CBCT scan. Sci Rep 10:1–13
32. Vandevoorde C, Franck C, Bacher K et al (2015) γ-H2AX foci as in vivo effect biomarker in children emphasize the importance to minimize x-ray doses in paediatric CT imaging. Eur Radiol 25:800–811
33. Jafarpour SM, Salimian M, Mohseni M et al (2018) Evaluation of ameliorative potential of vitamins E and C on DNA double strand break (DSB) in patients undergoing computed tomography (CT): a clinical study. Int J Mol Cell Med 7:226–233
34. Tao SM, Zhou F, Schoepf UJ et al (2019) The effect of abdominal contrast-enhanced CT on DNA double-strand breaks in peripheral blood lymphocytes: an in vitro and in vivo study. Acta radiol 60:687–693
35. Basheerudeen SAS, Kanagaraj K, Jose MT et al (2017) Entrance surface dose and induced DNA damage in blood lymphocytes of patients exposed to low-dose and low-dose-rate X-irradiation during diagnostic and therapeutic interventional radiology procedures. Mutat Res Genet Toxicol Environ Mutagen 818:1–6
36. Beels L, Werbrouck J, Thierens H (2010) Dose response and repair kinetics of γ-H2AX foci induced by in vitro irradiation of whole blood and T-lymphocytes with X-and γ-radiation. Int J Radiat Biol 86:760–768
37. Sharma PM, Ponnaiya B, Taveras M et al (2015) High throughput measurement of γH2AX DSB repair kinetics in a healthy human population. PLoS ONE 10:1–18
38. Cherednichenko O, Pilyugina A, Nuraliev S (2022) Chronic human exposure to ionizing radiation: individual variability of chromosomal aberration frequencies and G0 radiosensitivities. Mutat Res Genet Toxicol Environ Mutagen 873:503434. https://doi.org/10.1016/j.mrgentox.2021.503434
39. Vandevoorde C, Gomolka M, Roessler U et al (2015) EPI-CT: in vitro assessment of the applicability of the γ-H2AX-foci assay as cellular biomarker for exposure in a multicentre study of children in diagnostic radiology. Int J Radiat Biol 91:653–663
40. Kuefner MA, Brand M, Ehrlich J et al (2012) Effect of antioxidants on X-ray-induced γ-H2AX foci in human blood lymphocytes: preliminary observations. Radiology 264:59–67
41. Ding D, Zhang Y, Wang J et al (2016) Induction and inhibition of the pan-nuclear gamma-H2AX response in resting human peripheral blood lymphocytes after X-ray irradiation. Cell Death Discov 2:1–10
42. Kawamura K, Qi F, Kobayashi J (2018) Potential relationship between the biological effects of low-dose irradiation and mitochondrial ROS production. J Radiat Res 59:ii91–ii97
43. Byrne HL, McNamara AL, Domanova W et al (2013) Radiation damage on sub-cellular scales: beyond DNA. Phys Med Biol 58:1251–1267
44. Kim EM, Yang HS, Kang SW et al (2008) Amplification of the γ-irradiation-induced cell death pathway by reactive oxygen species in human U937 cells. Cell Signal 20:916–924
45. Das S, Joshi MB, Parashiva GK, Rao SBS (2020) Stimulation of cytoprotective autophagy and components of mitochondrial biogenesis / proteostasis in response to ionizing radiation as a credible pro-survival strategy. Free Radic Biol Med 152:715–727
46. Franco A, Sorriento D, Gambardella J et al (2018) GRK2 moderates the acute mitochondrial damage to ionizing radiation

exposure by promoting mitochondrial fission/fusion. Cell Death Discov 4:25. https://doi.org/10.1038/s41420-018-0028-7
47. Shimura T, Nakashiro C, Narao M, Ushiyama A (2020) Induction of oxidative stress biomarkers following whole-body irradiation in mice. PLoS ONE 15:1–13
48. Bartoletti-Stella A, Mariani E, Kurelac I et al (2013) Gamma rays induce a p53-independent mitochondrial biogenesis that is counter-regulated by HIF1α. Cell Death Dis 4:1–11
49. Maremonti E, Brede DA, Olsen AK et al (2020) Ionizing radiation, genotoxic stress, and mitochondrial DNA copy-number variation in Caenorhabditis elegans: droplet digital PCR analysis. Mutat Res Genet Toxicol Environ Mutagen 858–860:503277. https://doi.org/10.1016/j.mrgentox.2020.503277
50. Malakhova L, Bezlepkin VG, Antipova V et al (2005) The increase in mitochondrial DNA copy number in the tissues of gamma-irradiated mice. Cell Mol Biol Lett 10:721–732
51. Nugent S, Mothersill CE, Seymour C et al (2010) Altered mitochondrial function and genome frequency post exposure to γ-radiation and bystander factors. Int J Radiat Biol 86:829–841
52. Murphy MP, Bayir H, Belousov V et al (2022) Guidelines for measuring reactive oxygen species and oxidative damage in cells and in vivo. Nat Metab 4:651–662
53. Pajic J, Rovcanin B (2021) Ionizing radiation-induced genotoxic and oxidative damage in peripheral lymphocytes and plasma of healthy donors. Mutat Res Genet Toxicol Environ Mutagen 863–864:503313. https://doi.org/10.1016/j.mrgentox.2021.503313
54. Kohanoff J, Artacho E (2017) Water radiolysis by low-energy carbon projectiles from first-principles molecular dynamics. PLoS ONE 12:1–11
55. Shimura T, Koyama M, Aono D, Kunugita N (2019) Epicatechin as a promising agent to countermeasure radiation exposure by mitigating mitochondrial damage in human fibroblasts and mouse hematopoietic cells. FASEB J 33:6867–6876
56. Zhu W, Xu J, Ge Y et al (2014) Epigallocatechin-3-gallate (EGCG) protects skin cells from ionizing radiation via heme oxygenase-1 (HO-1) overexpression. J Radiat Res 55:1056–1065
57. Tubiana M, Feinendegen LE, Yang C, Kaminski JM (2009) The linear no-threshold relationship is inconsistent experimental data. Radiology 251:13–22
58. Siegel JA, Greenspan BS, Maurer AH et al (2018) The BEIR VII estimates of low-dose radiation health risks are based on faulty assumptions and data analyses: a call for reassessment. J Nucl Med 59:1017–1019
59. Chien L, Chen WK, Liu ST et al (2015) Low-dose ionizing radiation induces mitochondrial fusion and increases expression of mitochondrial complexes I and III in hippocampal neurons. Oncotarget 6:30628–30639
60. Tsapaki V (2020) Radiation dose optimization in diagnostic and interventional radiology: current issues and future perspectives. Physica Med 79:16–21
61. Panick C, Wunderle K, Sands M, Martin C (2018) Patient radiation dose reduction considerations in a contemporary interventional radiology suite. Cardiovasc Intervent Radiol 41:1925–1934
62. Morris PP, Geer CP, Singh J et al (2018) Radiation dose reduction during neuroendovascular procedures. J Neurointerv Surg 10:481–486
63. United Nations (2013) Scientific committee on the effects of atomic radiation. Sources, effects and risks of ionizing radiation : United Nations scientific committee on the effects of atomic radiation : UNSCEAR 2013 report to the general assembly with scientific annexes. Vol. II. Scientific Annex B. The effects of radiation exposure of children, New York
64. Hogarth K, Tarazi D, Maynes JT (2023) The effects of general anesthetics on mitochondrial structure and function in the developing brain. Front Neurol 14:1179823. https://doi.org/10.3389/fneur.2023.1179823
65. Coghlan M, Richards E, Shaik S et al (2018) Inhalational anesthetics induce neuronal protein aggregation and affect ER trafficking. Sci Rep 8:5275. https://doi.org/10.1038/s41598-018-23335-0

Authors and Affiliations

Kaley A. Hogarth[1,2] · Nicholas A. Shkumat[5,6] · Simal Goman[5] · Afsaneh Amirabadi[5] · Suzanne Bickford[5,7] · Prakash Muthusami[5,6,7] · Bairbre L. Connolly[5,6,8] · Jason T. Maynes[1,2,3,4]

✉ Kaley A. Hogarth
kaley.hogarth@sickkids.ca

✉ Bairbre L. Connolly
bairbre.connolly@sickkids.ca

✉ Jason T. Maynes
jason.maynes@sickkids.ca

[1] Program in Molecular Medicine, SickKids Research Institute, Toronto, ON, Canada

[2] Department of Anesthesia and Pain Medicine, The Hospital for Sick Children, 555 University Ave, Toronto, ON M5G 1X8, Canada

[3] Department of Anesthesiology and Pain Medicine, University of Toronto, Toronto, ON, Canada

[4] Department of Biochemistry, University of Toronto, Toronto, ON, Canada

[5] Department of Diagnostic and Interventional Radiology, The Hospital for Sick Children, Toronto, ON, Canada

[6] Department of Medical Imaging, University of Toronto, Toronto, ON, Canada

[7] Paediatric Neurovascular Program, The Hospital for Sick Children, Toronto, ON, Canada

[8] Medical Imaging, Hospital for Sick Children, 555 University Ave, Toronto, ON M5G 1X8, Canada